1

OIL FLOW VISUALIZATION ON VEHICLE MODELS IN SUPERSONIC FLOWS

Junich NODA, Atsushi TATE, Hideo SEKINE,
Mitsunori WATANABE, Takashi YOSHINAGA
Aerodynamics Division
National Aerospace Laboratory
Chofu-City, Tokyo, Japan

Nobuyuki TSUBOI, Masaru KODAMA, Takeshi KAEDA,
Keiji SATO, Hideki NOMOTO
Mitsubishi Heavy Industry Co., Ltd
Nagoya, Japan

SUMMARY

Flow visualization on the surface of an advanced aircraft or a supersonic transport and other vehicle models has been carried out using the supersonic wind tunnel of the National Aerospace Laboratory with the test section of 1 m× 1 m. In the present flow visualization study, (1) the application methods of a mixture of oil and pigment such as an oil dots method and an oil film method, (2) the effect of the property of oil on streak lines using silicone oil and paraffin oil (liquid paraffin), (3) a print method to obtain panoramic view on a circular cylinder, and (4) a liquid crystal method have been examined. Oil film method is found to be advantageous than oil dots method in supersonic flow. Paraffin oil draws streaks, while silicone oil draw no streaks. Liquid crystal did not visualize the necklace vortices in front of the engine nacelles.

I. INTRODUCTORY REMARKS

I-1. Flow Visualization Methods in Supersonic Flow

To find the features of the surface oil flow visualization on a vehicle model installed in the NAL 1 m× 1 m supersonic wind tunnel, we have tested several materials and methods.

(1) An oil dots method and an oil film method using machine oil and Titanium dioxide (TiO_2) as pigment (1992) were tested.

(2) The visualization of surface streak lines, separation lines and reattachment lines using two kinds of oils: silicone oil with a typical low surface tension coefficient and paraffin oil with a large tension coefficient, with carbon black as pigment (1993).

(3) A print method was developed to take the flow pattern of oil on a sheet of soft paper (1993).

(4) The possibility of visualizing the necklace vortices produced on the wing surface in front of the engine nacelles was examined by a liquid crystal method (1994).

I-2. The Features of Each Method

(1) Oil Dots Method [1]

A mixture of high viscous oil and pigment is used. The oil mixture is dotted with a brush by hand or with a special tool to supply a constant amount as a dot. Flow direction is easily defined. If dots are of the same size we can qualitatively infer whether or not the shear stress is great by the length of traces. The defect of this method is that it takes time to plot dots for preparation.

(2) Oil Film Method

A mixture of high viscosity oil and pigment is applied by patting the model surface with a sponge so that the thickness becomes fairly constant. The direction of the surface flow is visible but the magnitude of the shear stress is roughly estimated only through the thickness of the remaining mixture after the blow down. Depending on the kind of oil streaks appear.

(3) Print Method

We have developed a print method to press the oil flow pattern of a circular cylinder on a piece of paper so that it visualizes the panoramic surface flow pattern of a 360 deg roll angle. We also applied the method to visualize the internal surface flow of a channel such as a intake model of a supersonic transport engine, where we cannot take photographs of the flow pattern on the side wall as a projection without distortion.

(4) Liquid Crystal Method [2,3,4]

We have tested a liquid crystal to define the separation line of the necklace vortices in front of the engine nacelles utilizing the recovery temperature drop. The liquid crystal reflects lights of particular wave lengths depending on the temperature of it

In the following section we show the results of experiments conducted for each year.

I-3. Wind Tunnel and Models

The flow visualization was conducted on the surface of a supersonic transport model (0.7315 m) and other supersonic vehicle models and on the wind tunnel wall using the NAL 1 m×1 m supersonic wind tunnel. The Mach number range of this wind tunnel is from 1.4 to 4.0. The Reynolds number ranges from 2 to 5×10^7 per 1 meter. Dynamic pressure varies between 65 and 155kPa. The duration of the flow reaches a maximum of 40 s.

II. OIL DOTS METHOD AND OIL FILM METHOD (1992)

II-1. Introduction

The surface flow of a model is often visualizing by an oil dots method[1] or an oil film method. In the oil dots method the surface of a model is dotted with a mixture of oil and pigment using a small brush or a special tool to push out the same amount of oil per dot. After the blow down of the wind tunnel, each oil dot draws a trace of some distance downstream by the skin friction of the surface flow from the upstream region. The length of a trace roughly corresponds to the magnitude of the shear stress. The direction of the trace shows the direction of the shear stress at that point. Because the friction in a hypersonic wind tunnel is smaller than in a conventional blow-down supersonic wind tunnel, the overlapping of the traces in a hypersonic wind tunnel test is more easily controlled than in the supersonic wind tunnel test by selecting the viscosity of oil. The oil dots method is, therefore, often used in hypersonic flow to visualize blunted models such as a Gemini type reentry vehicle.

The purpose of the present experiment is to compare both methods on a supersonic transport model in a supersonic flow using the same mixture of machine oil and titanium dioxide (TiO_2). The flow visualization is intended to find out; 1) how the separation occurs at the end of the wings, how the shock boundary layer interference occurs between the engine and the wings, and how the separation of the vortices along the streak affect the flow on the wings. Another purpose is to observe 2) how the artificial roughness produce the flow downstream.

II-2. Application of Oil Mixtures

We applied dots of a mixture of machine oil and the powder of TiO_2 (white) using a tool to supply a constant volume dot (AD7000Z controller, made by

Iwashita Eng. Co.) to the upper left side of the supersonic transport model (horizontal main wing and vertical and horizontal tail wings) . On the other hand, we coated the right side of the supersonic transport model with the oil mixture by tapping the surface with a sponge. We prepared the model to test the oil film method and the oil dots method at the same time as shown in Fig. 1. After exposing the model at an angle of attack of α =8.7 deg to the flow of M_∞=2.03, we took a photograph of oil flow patterns on the model. Fig. 2. shows the oil flow on the main wings, and Fig.3 shows the oil flow pattern on the vertical tail plane.

II-3. Results of Experiment

(1) Comparison of the Two Methods

Because of the large shear stress acting on the surface of the wing the oil mixture of the dots drew long traces, which overlapped each other. As a result, the distance of a trace becomes vague and only the direction of the oil flow is found. This pattern helps roughly overview the whole flow pattern on the wing. On the other hand, the oil film method shows details of the flow direction, which are clearer than the one by the dots method. To avoid damage by a large load on the model and on the sting at the start of blows, the supersonic wind tunnel is usually started holding the angle of attack at α =0 deg. After the supersonic flow is established, the angle of attack of the model is varied to the test angle $\alpha = \alpha_0$ deg. Thus, in the oil dots method the traces draw some distance during the time at α =0 deg. The traces begin to draw different directions at $\alpha = \alpha_0$. As the results traces blur or overlap on the former traces during the test time at $\alpha = \alpha_0$ deg. This overlap of traces sometimes confuses the judgement of the flow direction when we use an oil mixture with low viscosity. The blur of the trace by the dots method in Fig.2 and Fig.3 is caused by this difference of flowing directions of traces at α =0 deg and at $\alpha = \alpha_0$. On the other hand in the oil film method usually the former pattern at α =0 deg is wiped away when the test time at $\alpha = \alpha_0$ deg is greater than the build-up time of the flow at α =0 deg. In Fig.2 both methods show separation lines and reattachment line of vortices produced by the streaks upstream, and the vortices originated at the junctions of streaks and the main wings.

(2) Artificial Roughness along the Leading Edges

To promote the transition of the boundary layer on the model surface small disks of 2 mm diameter are attached in line along the leading edges of the wings as shown in Figs. 2 and 3 and near the nose of the fuselage. About 10 to 20 times the diameter of the disk downstream from the disks, the oil flow draws similar streaks. The streaks, then, changes to blur, where the transition to turbulent boundary layer seems to occur. This transition is clearly identified by the oil film method. From the present experiments, the oil film method draws better flow patterns of transition than by the dots method.

II-4. Supplementary Experiments

In Fig. 3 oil streaks starting from the upstream region of the roughness disks never make contact with the disks. After making detours around the disks the streaks draw downstream. To examine the detour of streaks around a disk we conducted a supplementary experiment utilizing the boundary layer on the wall of the supersonic wind tunnel 1 m downstream of the test section. Although the boundary layer with a thickness of about 80 mm is turbulent, there is a laminar subboundary layer close to the wall. The 14 disks of 10 mm diameter and 1 mm thickness are attached to the wall in line at intervals of 20 mm, as shown in Figs. 4 and 5. Four disks are overlapped on the two figures. To obtain flow pattern around the disks we applied a mixture of paraffin and TiO_2 with a couple of drops of oleic acid as belts 30 mm in width on the upstream region and downstream region parallel to the disks. The test was conducted at Mach number

3.0.

Fig. 4 shows that the streaks of the mixture in front of the disks always detour them making necklace vortices. This is the same as what we observed on the edges of the wings. The fine streaks appear downstream at a point 25 times of the diameter of disk.

Fig. 5 shows that turbulent wedges exist just behind the disks, where the oil mixture is wiped away about 4 times diameter downstream by large shear stress. A white region follows the wiped region, where fine lines suddenly mixed with each other. As the oil mixture flows further downstream steaks begin to appear again. This is the feature of paraffin when it is used for oil flow visualization. This pattern is similar to what we have observed around and behind the 2 mm diameter disks as roughness on the supersonic transport model. When we used silicone oil instead of paraffin these fine long trace does not appear as, will be shown next.

II-5. Conclusions

(1) An oil film method is advantageous than an oil dots method in supersonic flow to make a surface flow visible..

(2) Paraffin oil tends to make streaks on surface flow, while silicone oil does not.

III. TRACES OF SILICONE AND PARAFFIN OILS (1993)

III-1. Introduction

In studying the oil flow visualization of a supersonic transport model in 1992 we found that an oil film method is superior to an oil dots methods in the supersonic flow regime. In 1993 we have studied surface flow patterns of several vehicle models using the oil film method. This study include models of the Orbital Reentry Experiment vehicle (OREX) and circular cylinders at high angles of attack where a side force acts. For circular cylinders we developed a printing method which demonstrated panoramic views of the flow pattern around the cylinders.

III-2. Experimental Methods

Because the one shot view of a photograph is limited to a certain area of a 3-dimensional model, the photographs of oil flow patterns of circular cylinder models at high angles of attack do not show the whole flow pattern on the models at one time. To observe the oil flow pattern as a panoramic one, we tried printing the pattern on a piece of paper by wrapping the cylinder with it.

III-3. Results of Experiment

(1) Skin Friction Traces on the Wall

It is well known that the surface tension coefficient of oil affect the oil flow pattern in flow visualization. By a print method, we examined the effect of the surface tension coefficients of oils on the oil flow traces. Two kinds of oils, silicone (500cs) and paraffin oils, were tested, because the surface tension coefficient of silicone oil is smaller than that of paraffin oil. We mixed each oil with carbon black powder. We applied thin coats of each oil mixture to the wind tunnel wall by tapping it with a sponge brush, then we exposed the wall to a flow of Mach 2.0 for 20s. We print these patterns on two sheets of soft paper by pressing them on the wall. The paper is the type generally used to cover sliding doors, being the goods on the market. Fig. 6(a) is a pattern made by a mixture of silicone oil and carbon black, which shows the flow pattern made only behind the disks attached for roughness. On the other hand, Fig. 6(b) is a pattern made by a mixture of paraffin and carbon black with the same disks upstream, showing fine streaks indicating the surface flow direction. Comparing these figures, it can be seen that to visualize the flow

direction on a model paraffin oil works better than silicon oil. The property of paraffin oil to draw streaks, however, acts to destroy a bubble or separation line, as shown next.

(2) Visualization on a Reentry Capsule Model

Oil flow visualization on the surface of a model of the Orbital Reentry Experiment vehicle (OREX) is conducted using silicone and paraffin oils at Mach number M_∞=3.0.[5] The contour of the OREX model is composed of a spherical nose section of 50 mm radius and a following conical flare of 113.3 mm diameter with an apex half angle of 50 deg. The first derivatives of the two curved surfaces at the joint line are the same; however, the second derivatives are different. If we assume that there is no friction, the velocity is accelerated downstream on a spherical nose, while the velocity on a cone surface with constant half apex angle is constant. Thus, some irregular flow field will occur at the junction line of the two shapes.

Fig. 7(a) shows a photograph of oil flow visualization made by a mixture of silicone oil and titanium dioxide (TiO_2). There are no visible streaks; however, at the joint line the oil mixture stopped once, forming a thick circle. The thickness suddenly becomes thin toward the downstream region. It seems that the laminar boundary layer separated once at the joint line. The real cause of the ring is not known yet.

Fig. 7(b) shows the oil flow visualization of the same model using a mixture of paraffin oil and titanium dioxide (TiO_2), where the streaks or skin friction lines appear clearly. The oil mixture once deposits near the joint line as a ring; however, the streaks pass the ring downstream. In this case the streaks have the effect of letting the oil mixture break through the ring and flow downstream. A clear difference is observed between the two oil mixtures.

(3) Visualization of Separated Flow on Circular Cylinders [6]

Fig. 8(a) is a schlieren photograph of a circular cylinder at an angle of attack of α=25 deg in a free stream Mach number M_∞=2.02 ($Re_\infty = 1.26 \times 10^7$ based on the length). In spite of the axisymmetric shape of the model side force acts due to the asymmetric separation of vortices behind the cylinder. Fig. 8(b) shows the separation lines and reattachment lines of vortices visualized by a mixture of paraffin oil and TiO_2, where the large shear stress regions are visualized. This photograph is not enough to tell how the side flow behaves.

To obtain the whole flow pattern around the cylinder surface we employed a printing method. After we exposed the cylinder coated to an oil mixture in the supersonic flow for a certain time at a constant α, we stopped the flow without changing the angle of attack α of the model. We gently wrapped the cylinder with a sheet of soft paper, pattern was printed on the paper as a panoramic view for a roll angle of $0 < \phi < 360$ deg.

Fig. 9(a) shows a printed skin friction flow pattern using a mixture of silicone oil and carbon black on a circular cylinder 400 mm in length and 54 mm in diameter. The experiment was carried out at α=15 deg, for M_∞= 1.77 with the Reynolds number 1.12×10^7 based on the cylinder length. Because we visualized the cylinder using silicone oil, only the separation lines are observed. The angle of attack of α=15 deg is not so large as to produce an asymmetric separation, thus, the flow pattern is symmetric with respect to the meridian line of 180 deg, showing that the side force is not acting.

Fig. 9(b) shows the separation lines of the same cylinder model at an angle of attack of 25 deg for M_∞=1.77 with the Reynolds number 1.06×10^7. The secondary separation line on the left side shifts to the meridian line of 180 deg, thus the side force is acting under this flow condition.

Fig. 10(a) shows a printed flow pattern on an ellipsoidally blunted cylinder visualized with the mixture of paraffin oil and carbon black at α=27 deg for M_∞=1.5. The blunted nose diameter ratio of the cylinder is a/b=1/6, where a is the diameter of the ellipsoidal nose shape in the axial direction and b is the

diameter in the radial direction. Detailed streaks of the skin friction line are observed. Since the flow pattern is symmetric, this figure means that side force is not acting.

Fig. 10(b) shows a printed flow pattern on the same ellipsoidally blunted cylinder at α = 28 deg for Mach number M_∞=1.61. The flow pattern is similar to Fig. 9(b), showing the asymmetric separation of the secondary separation line on the left side of the cylinder. This suggests that side force is acting.

III-4. Conclusions

An oil film method was tested using paraffin oil and silicone oil for the surface flow visualization of models in supersonic flows.

(1) Paraffin oil tends to make streaks on the models, making the surface flow direction clear. Silicone oil does not draw streaks.

(2) A print method visualizes the panoramic view of separation lines and reattachment lines on the surface of a cylindrical body.

IV. Surface Flow Visualization with Liquid Crystal (1994)

IV-1. Introduction

Surface flow visualization with a mixture of oil and pigment is a conventional and simple method to demonstrate the flow pattern on a model. The method requires coating with the mixture at each time the wind tunnel is blown. To save time and work for the preparation we tried using tested liquid crystals to visualize the flow pattern on a vehicle model. As a coating, liquid crystal is enclosed in microcapsules surrounded by Arabian gum and gelatin. The liquid crystal changes the wave length of reflecting light at particular temperatures. Before we apply a coat of the liquid crystal to the surface of a model we apply a black coating to the model to prevent the reflection of light which reaches the model surface through the liquid crystal coat. By observing the time-dependent variation of the color on the model surface, we can define the local variation of the temperature on the model. This method has demonstrated the measurement of the heating rate on a vehicle model in a hypersonic wind tunnel. The recovery factor and the recovery temperature on a model depend on whether the flow is laminar or turbulent. Utilizing this difference, some researchers have shown that liquid crystal is useful in visualizing turbulent wedges, separation lines and transition lines on the surface of a wing model in the transonic region by selecting suitable phase change temperatures of liquid crystals[2, 3, 4].

In the present experiment, we have conducted tests to determine out whether liquid crystal is useful in visualizing the flow pattern on a total supersonic transport model. This is based on the fact that the adiabatic recovery temperature on the model surface is lower than the stagnation temperature of the air stored in the tank and the recovery temperature on the wall is different, depending on whether the flow is laminar or turbulent and on the local heat transfer rate. The necklace vortices produced on the main wings in front of the engines are the focus of our test.

IV-2. Model and Liquid Crystal

We have utilized the lower side of a supersonic transport model to visualize temperature variations with liquid crystal. Since this model is fabricated to measure the aerodynamic forces by six-force balance, a number of small disks 2 mm in diameter are attached in line as roughness on the leading edges of wings and on the nose section of the fuselage to simulate the turbulent boundary layer in the real flight of a transport. We applied a black coating (SSM-8, made by Nippon Capsule Products) to the model to prevent reflection of light on the model metal surface. After the black coating was completely dry we applied a coating of the liquid crystal (RM-02, made by the same company). The color

change temperatures are -1.2, 0.1, 1.0, 2.3 and 3.1 deg C, for which different colors correspond. These specimens are shown later. In Fig. 12 the coated transport model is shown. We recorded the color change of the transport model in wind tunnel tests with on an 8 mm video camera. Later we printed out the typical frames of the color change with a video printer.

IV-3 .Results and Discussions

We carried out the experiment three times at the angle of $\alpha = 0^\circ$.

Test run #	Re_∞	T_0(° C)	M_∞	Ta(° C)	L. crystal#
16182	2.151×10^7	17.5	2.02	14.2	RM02
16183	2.124×10^7	17.3	2.02	14.2	RM02
16184	2.117×10^7	17.3	2.01	14.3	RM02+RM810

Reference length is the total model length, ℓ=0.7315 m.

Figs. 13(a), (b), (c), (d), (e), (f) and (g) show the color change of the model during the wind tunnel test at Run #16183. Against our expectation the color change at the wings caused by the necklace vortices under the interaction of the boundary layer and the shock wave around the engine nacelles were not clearly demonstrated.

Fig. 13(b) shows the photograph at 5 s after the start of the blow. Judging from the color the temperature begins to drop at the leading edge of the main wings and at the edges of the engine nacelle. In Fig. 13(c) at 10 s the temperatures of the leading edge of strakes and the whole main wings begin to drop. In Fig. 13(d) at 15s the temperature begins to drop on the whole strake and the fuselage. As shown in Fig. 13(e) at 20 s and Fig. 13(f) at 23 s the fuselage temperatures finally begin to decrease. For reference Fig. 13(g) 20 s later from the end of the blow is shown. Because of the adiabatic expansion of the surrounding air the temperature of the model suddenly begins to drop. Thus the model suddenly changes color to that of a lower temperature. The correspondence of the color and the temperature is shown on the side of Fig. 13(g).

In these Figures, the interaction regions between the boundary layer and the shock wave due to the existence of the nacelles of the engines were not observed by color change. It seems that a difference of temperature large enough to change the color of the liquid crystal did not occur because the roughness is attached to the edge of the transport model to change the surface flow turbulent. We infer the reasons as follows:

The adiabatic recovery temperature T_{aw} is determined by a recovery factor r.

$$T_{aw}=T_\infty\{1+r(\gamma-1)\ M_\infty^2/2\} \qquad (1)$$

At a stagnation point r=1.0, thus $T_{aw}=T_0$. Generally, r< 1.0, so that,

$$T_0 = T_\infty\{1+(\gamma-1)\ M_\infty^2/2\}$$
$$\geqq T_\infty\{1+r(\gamma-1)\ M_\infty^2/2\}=T_{aw} \qquad (2)$$

Take Pr as the Prandtl number with the value Pr=0.72. For a laminar boundary layer, the recovery factor of a surface parallel to the free stream is $r=Pr^{0.5}$, yielding r=0.849, while for a turbulent boundary layer, the recovery factor is $r=Pr^{0.33}$, yielding r=0.896. In either case, the surface recovery temperature T_{aw} becomes lower than the stagnation temperature T_0 so that the surface temperature begins to fall after the wind tunnel blows. If a laminar boundary layer turns to a turbulent boundary layer on a surface across a certain border line upstream the engine nacelles the recovery factor r changes from 0.849 to 0.896. Consequently, the adiabatic recovery wall temperature T_{aw} in the turbulent region is higher than in the laminar region. The heating rate, however, becomes greater in the turbulent region than in the laminar region. Thus the surface

temperature in the turbulent region must have decreased faster than the laminar region across the border. A clear color difference must exist across the border if the dissipation of heat is small. In the present experiment, however, the boundary layer was artificially changed to turbulent by the roughness at the edge of the model and that the model was made of metal with a large heat conductivity. Consequently, a temperature difference caused by the change from the laminar boundary layer to the turbulent boundary layer does not exist so that the necklace vortices in front of the engine nacelle were not captured by the present liquid crystal method.

IV-4 .Conclusions

The liquid crystal method of observing the temperature difference was not useful in detecting the location of the necklace vortices in front of the engine nacelles on a transport model where the boundary layer is artificially changed to turbulent.

V. CONCLUDING REMARKS

Surface flow visualization of supersonic vehicles was conducted using silicone oil, paraffin oil and powders of titanium dioxide and carbon black. The visualization experiments concludes that:

(1) An oil film method is advantageous than an oil dots method in supersonic flow to make a surface flow visible.

(2) Paraffin oil tends to make streaks on surface flow, while silicone oil does not.

(3) A print method visualizes the panoramic view of separation lines, reattachment lines, and streaks of skin friction lines on the surface of a cylindrical body.

(4) The liquid crystal method of observing the temperature difference was not useful in detecting the location of the necklace vortices in front of the engine nacelles on a transport model where the boundary layer is artificially changed to turbulent.

REFERENCES

(1) Y. Yamamoto, M. Watanabe, S. Nomura, T. Koyama, K. Hozumi, A. Yoshizawa, T. Ito, and H. Takatuka; Oil Flow Patterns on a Series of Capsule-Type Reentry Vehicles at Hypersonic Speeds, NAL TM-557, Nov. 1986.

(2) N. Sudani,M. Sato, H. Kanda, and K. Matsuno; Flow Visualization Studies on Side wall Effects in Two-Dimensional Transonic Airfoil Testing; AIAA Paper 93-0090, January 1993.

(3) M. Noguchi, Y. Ishida, N. Sudani, M. Sato, and H. Kanda; Measurement of the Boundary Layer Transition Point over a 2-D LFC Airfoil in Transonic Flow Using Liquid Crystals, NAL TM-679, March 1995.

(4) T. Asanuma; Handbook for Flow Visualization (New ed.) Asakurashoten 1992.

(5) J. Noda, A. Tate, H. Sekine, M. Watanabe and T. Yoshinaga; Oil Flow Visualization on Bodies in Supersonic Flows, 26th Fluid Dynamics Conference (Japan), Oct., 1994.

(6) A. Tate, M. Watanabe, J. Noda, H. Sekine and T. Yoshinaga; Side Force Acting on Blunted Circular Cylinder Bodies at High Angles of Attack in Supersonic Flow, NAL TR-1255, Dec. 1994.

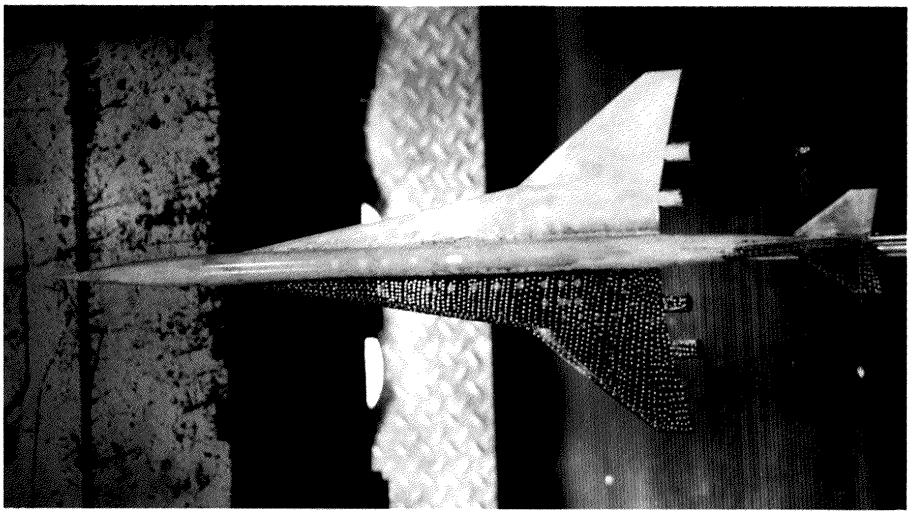

Fig.1 Preparation for surface flow visualization by an oil dots method (left) and an oil film method (right).

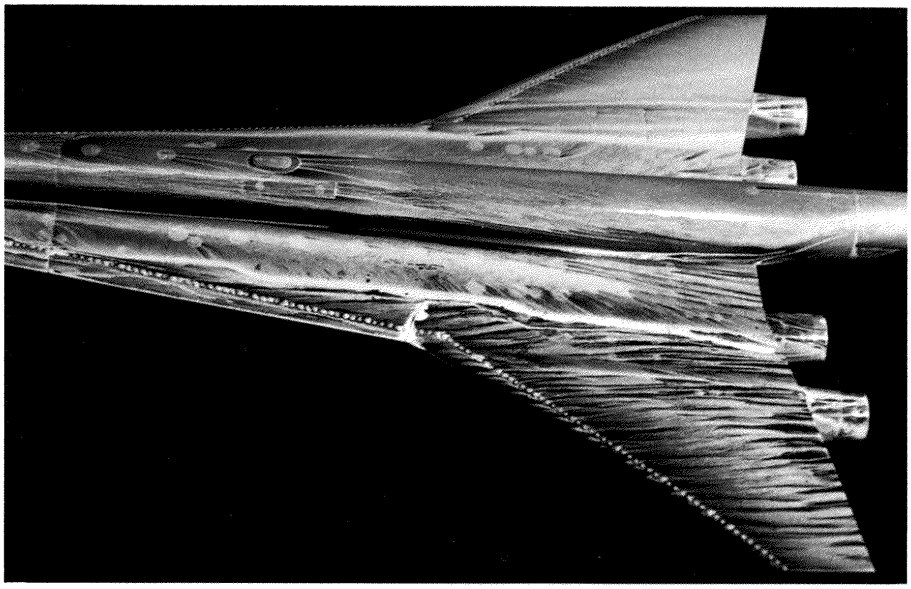

Fig.2 Oil flow visualization near the main wings.
Vortex separation lines, reattachment line on fuselage and transition after artificial roughness are visible.

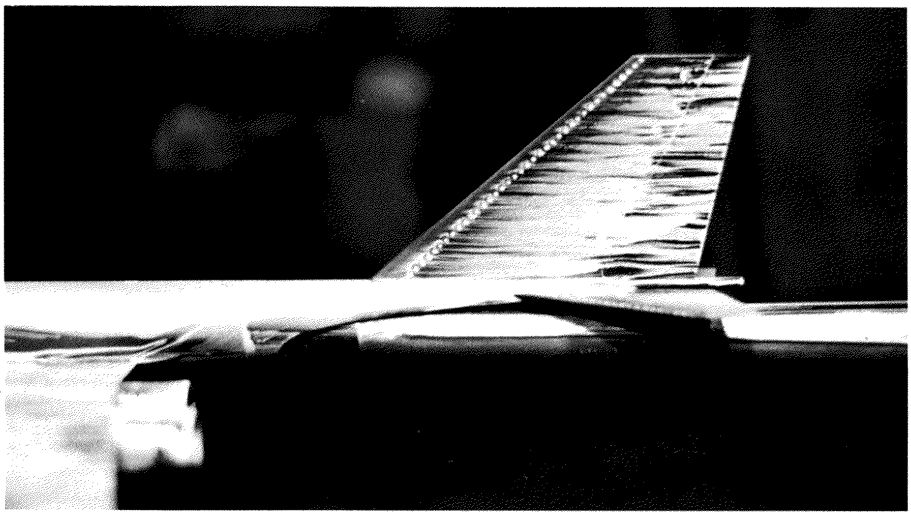

Fig.3 Flow Visualization near the vertical tail plane.
Note the flow around the artificial roughness.

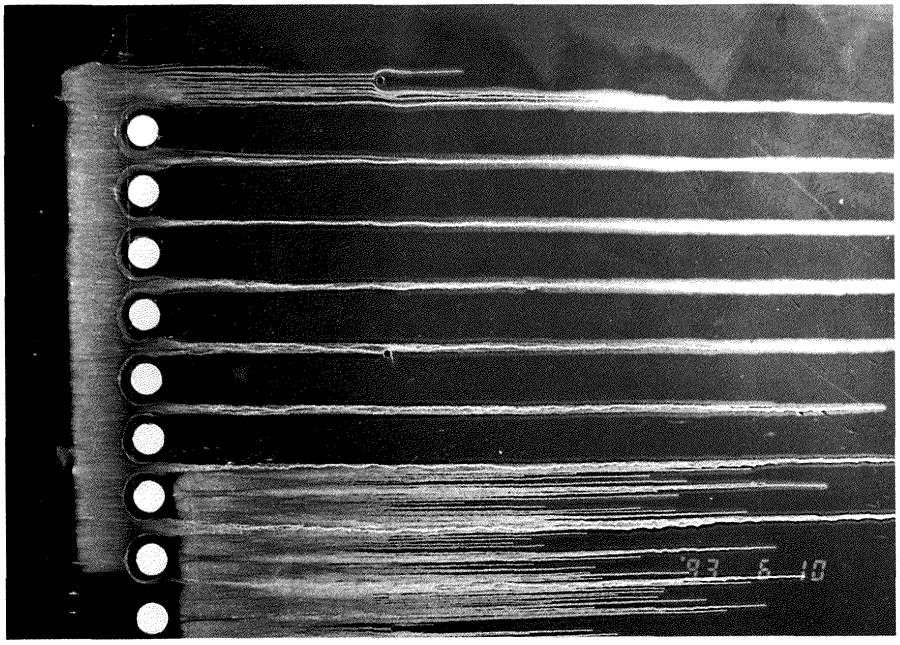

Fig.4 Simulation of roughness disks on the transport model using the wall of the supersonic wind tunnel (1m× 1m).
Disks 10mm ϕ with 1mm thickness are attached at 20mm intervals. The mixture of paraffin oil and TiO_2 is applied in front of the disks.

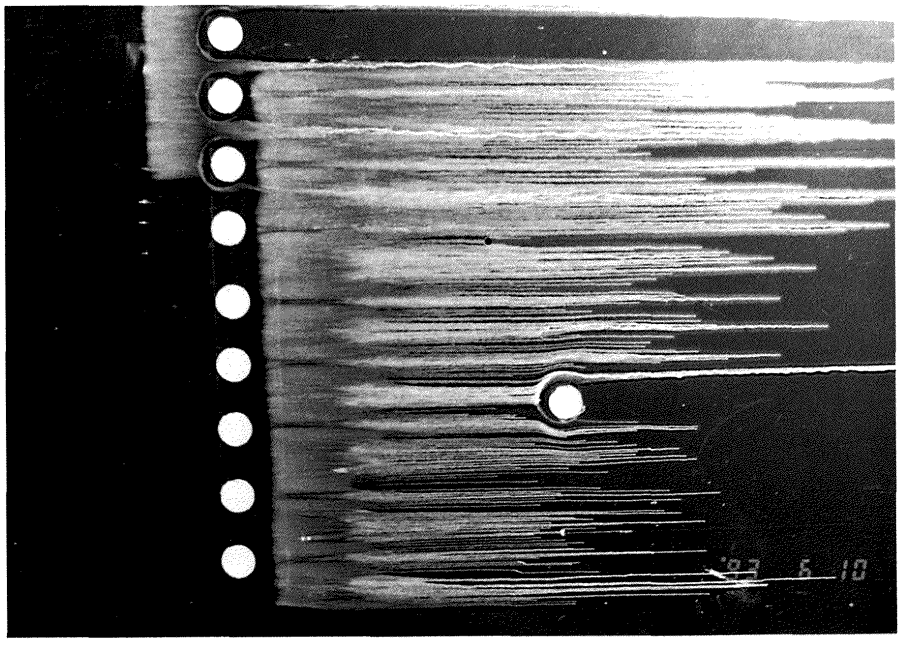

Fig.5 Simulation of roughness disks on the wall of the supersonic wind tunnel. Disks 10mm ϕ with 1mm thickness are attached at 20mm intervals. A mixture of paraffin oil and TiO_2 is applied behind the disks. Turbulent wedges appear after the disks wiping oil downstream.

Fig.6(a) Surface flow downstream of disks by a mixture of silicone oil and carbon black is printed on a sheet of soft paper. Streak is invisible. M_∞=2.0

Fig.6(b) Surface flow downstream of disks by a mixture of paraffin oil and carbon black is printed on a sheet of soft paper. Streaks are observed. M_∞=2.0

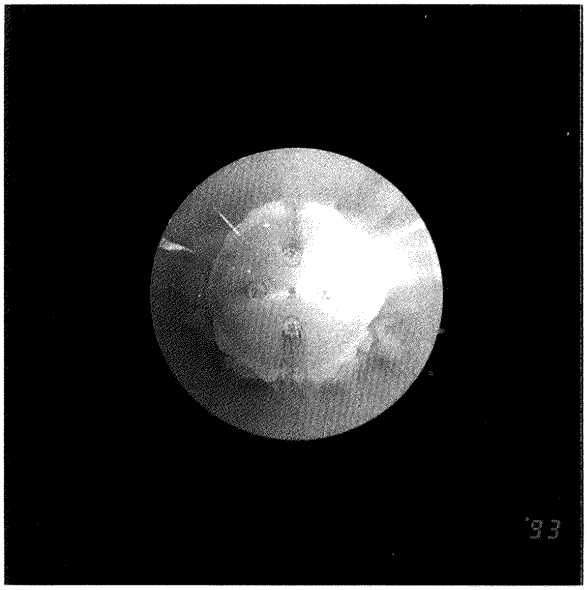

Fig.7(a) Surface oil flow on a Orbital Reentry Experiment vehicle (OREX) model using a mixture of silicone oil and TiO_2. A ring is observed at the junction line of curvatures.

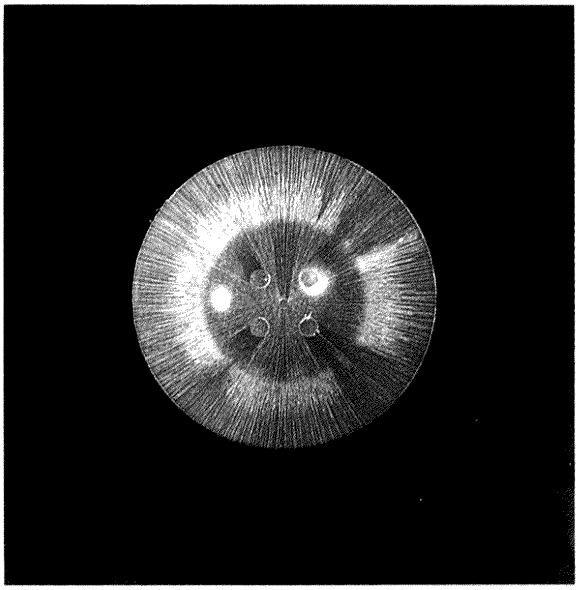

Fig.7(b) Surface oil flow on a Orbital Reentry Experiment vehicle (OREX) model using a mixture of paraffin oil and TiO_2. A ring is observed at the junction line of curvatures. Streaks wash the deposited mixture downstream.

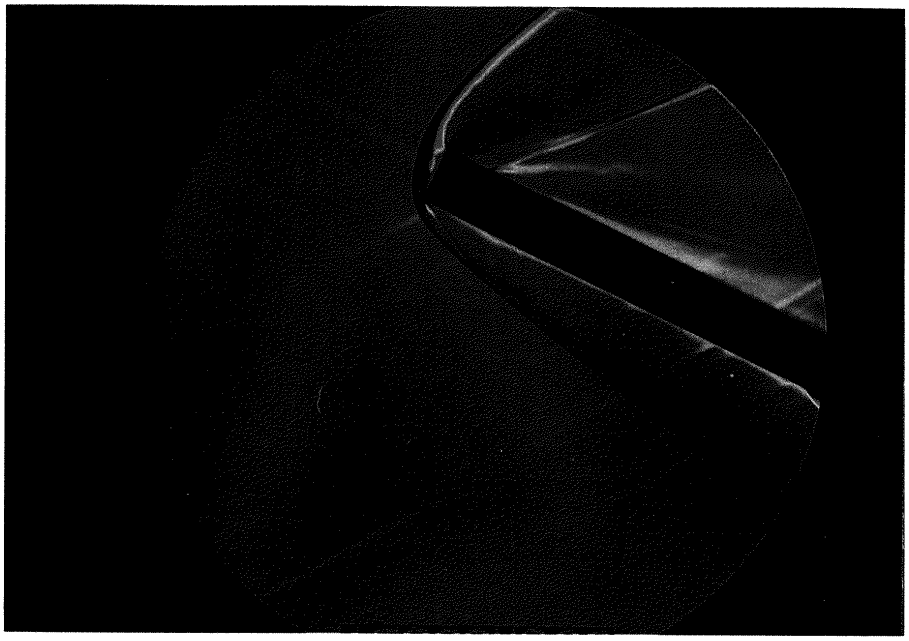

Fig.8(a) Schlieren photograph of a cylinder at α =25 deg for M_∞=2.02 (Re_∞=1.26× 10^7). Side force is acting.

Fig.8(b) Oil flow pattern on the lee side of the cylinder of Fig.8(a) with a mixture of paraffin oil and TiO_2. The separation lines on the sides and the reattachment region with large shear stress on the lee side are observed.

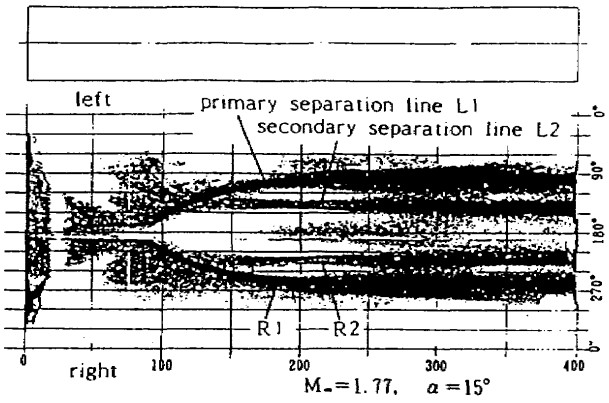

Fig.9(a) Printed figure of surface oil flow of a flat faced cylinder for roll angle $0 \leqq \phi \leqq 360$. Mixture of silicone oil and carbon black is used. Separation lines are visible, however, streak is invisible. α =15 deg, M_∞=1.77, Re_∞= 1.12×10^7. No side force acts.

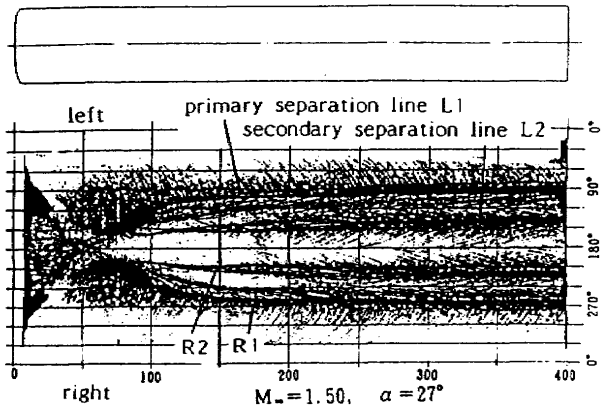

Fig.10(a) Printed figure of surface oil flow of an ellipsoidally blunted cylinder (b/a=1/6) for roll angle $0 \leqq \phi \leqq 360$. Mixture of paraffin oil and carbon black is used. Separation lines, reattachment lines and streaks are visible. α =27 deg, M_∞=1.50, Re_∞= 1.06×10^7.

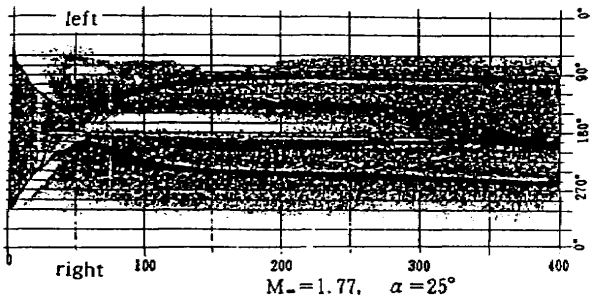

Fig.9(b) Printed figure of surface oil flow of a flat faced cylinder. Mixture of silicone oil and carbon black is used. Secondary separation lines are asymmetric, thus, side force is acting. α =25 deg, M_∞=1.77, Re_∞= 1.12×10^7.

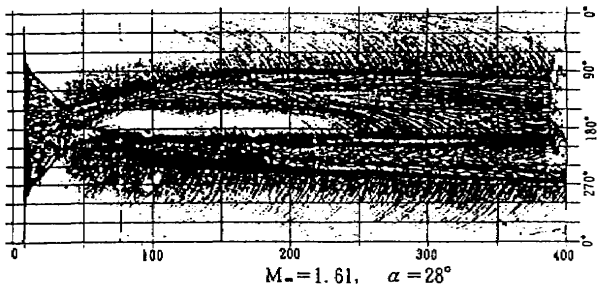

Fig.10(b) Printed figure of surface oil flow of an ellipsoidally blunted cylinder (b/a=1/6). Mixture of paraffin oil and carbon black is used. Separation lines, reattachment lines and streaks are visible. α =28 deg, M_∞=1.61, Re_∞= 1.06×10^7.

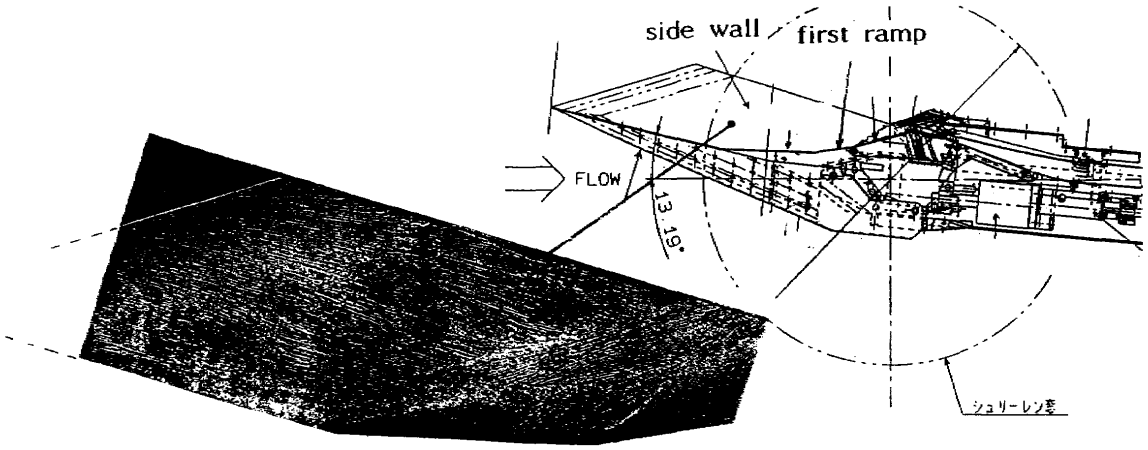

Fig.11 Visualization of side wall flow of supersonic engine intake model by print method at M_∞=3.5. Mixture of paraffin and TiO_2 is used. Shock wave boundary layer interaction from the first ramp corner is observed.

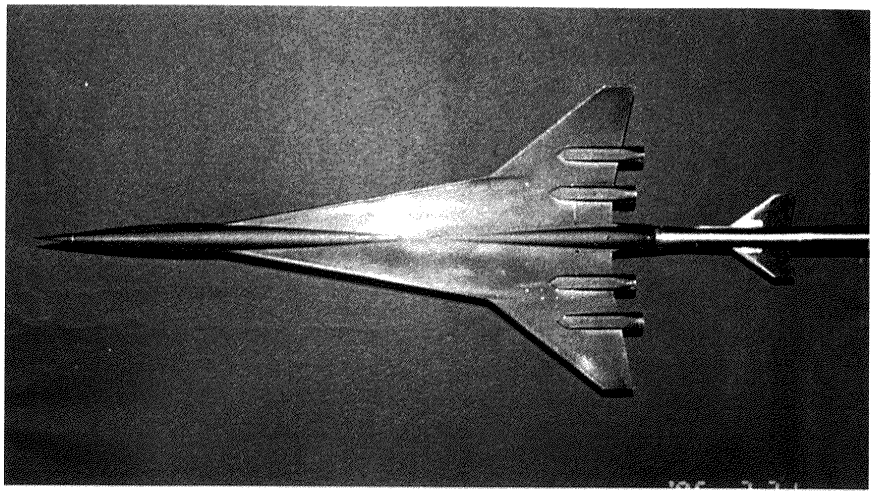

Fig.12 Lower side of supersonic transport model is coated with liquid crystal paint. Four engine nacelles are attached.

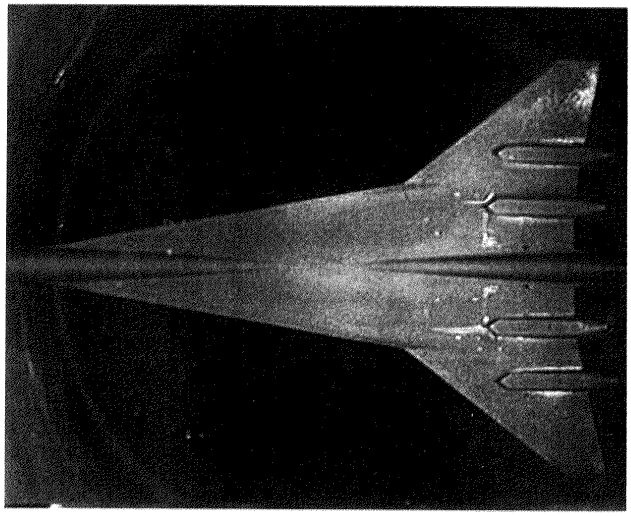

Fig.13(a) Transport model just before the blow at α =0 deg for M_∞=2.0, t=0s.

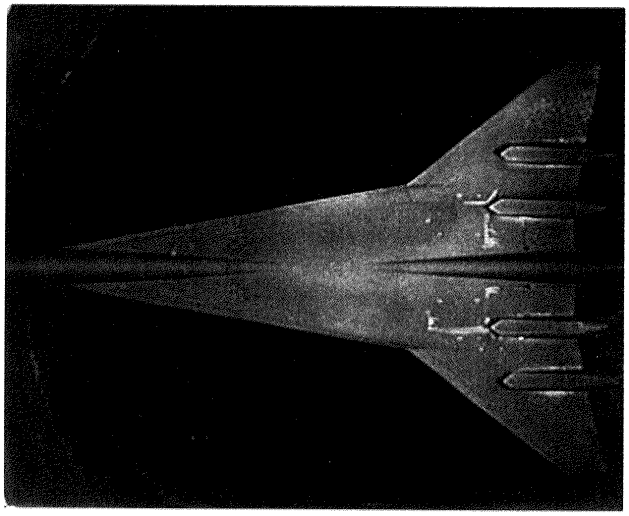

Fig.13(b) Transport model after the blow. t=5s.

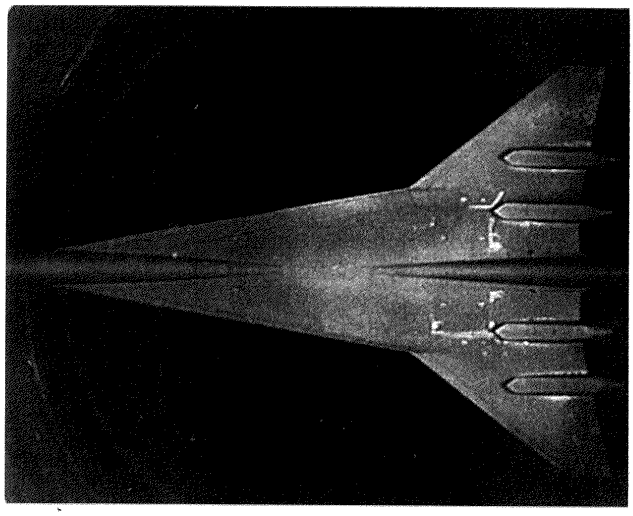

Fig.13(c) Transport model after the blow. t=10s.

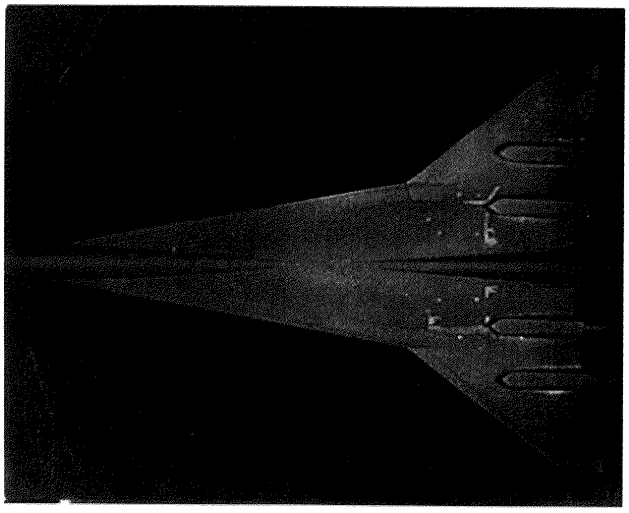

Fig.13(d) Transport model after the blow. t=15s.

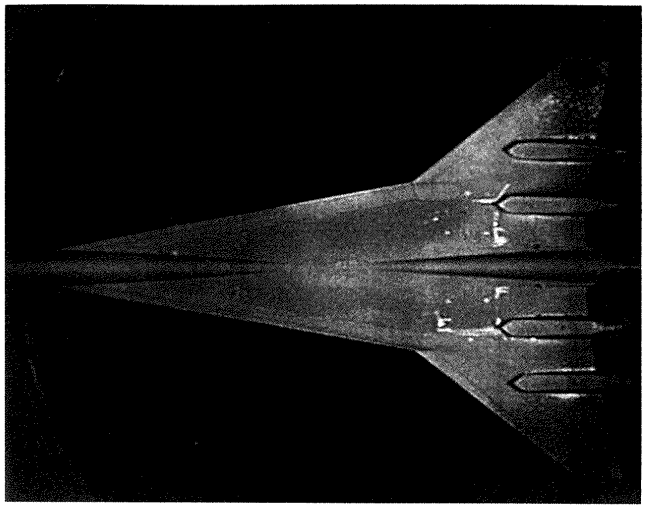

Fig.13(e) Transport model after the blow. t=20s.

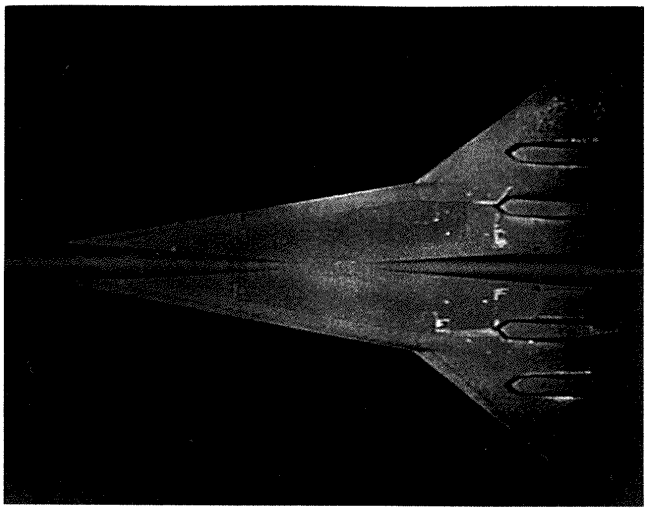

Fig.13(f) Transport model after the blow. t=23s.

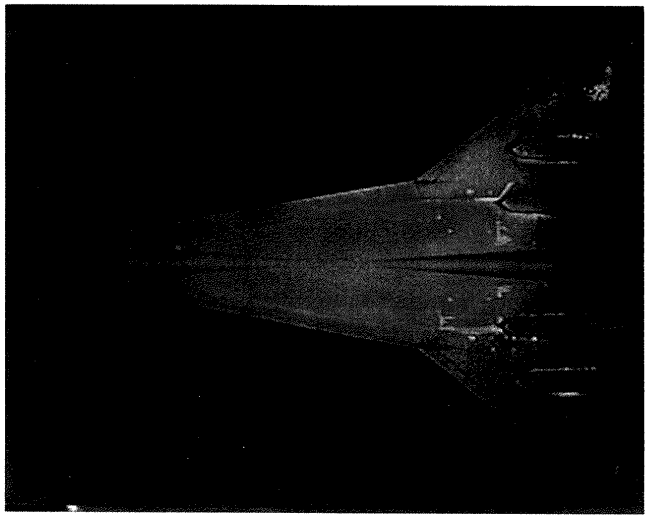

Fig.13(g) Transport model after the stop of the blow. t=20s.